1

2   DR. DEREK G. BOLSER (Orcid ID : 0000-0001-5880-1693)

3

4

6

7

Feature

Optic–acoustic Analysis of Fish Assemblages at Petroleum Platforms

Derek G. Bolser | Marine Science Institute, the University of Texas at Austin, 750 Channel View Drive, Port Aransas, TX, 78373 | Oregon State University, Cooperative Institute for Marine Resources Studies - Hatfield Marine Science Center, Newport, OR. Email: bolserd@oregonstate.edu

Jack. P. Egerton | Marine Science Institute, the University of Texas at Austin, Port Aransas, TX | Echology Ltd, Menai Bridge, Anglesey, UK

Arnaud Grüss | National Institute of Water and Atmospheric Research, Hataitai, Wellington, NZ

Brad E. Erisman[1,5] | Marine Science Institute, the University of Texas at Austin, Port Aransas, TX | National Oceanic and Atmospheric Administration, National Marine Fisheries Service, Southwest Fisheries Science Center, La Jolla, CA

8   **Abstract**

9   Petroleum platforms provide high-relief reef habitat in several ocean basins and are
10   important to fishes and fishers alike. To determine which variables were important for shaping
11   platform-associated fish assemblages on a basin-wide scale in the U.S. Gulf of Mexico, we
12   employed optic and acoustic methods to measure fish distribution (geographic and water-
13   column), abundance, biomass, density, size, diversity, and richness at 54 platforms. We found
14   that variables related to freshwater inflow and meso-scale circulation patterns (e.g., salinity)
15   affected more metrics than platform characteristics (e.g., platform depth). Platform fish
16   assemblages varied gradually along gradients of these variables instead of exhibiting distinct

17 assemblage groupings in non-metric multidimensional scaling space. These effects contributed to

18 the presence of biomass, density, diversity, and richness "hotspots" at platforms offshore of the

19 Atchafalaya River. Our findings underscore the importance of freshwater inflow and circulation

20 patterns in explaining variation in reef fish assemblages in the U.S. Gulf of Mexico.

21 **INTRODUCTION**

22   Petroleum platforms (hereafter platforms) are immensely popular fishing locations in

23 U.S. waters of the Gulf of Mexico (GOM), as they are easily located by fishers and provide a

24 unique form of relief and complexity among reef habitats in the region. Platforms support

25 abundant fish communities, and they allow fishes to redistribute vertically to avoid stressors

26 (e.g., hypoxia, predation) while remaining associated with refugia (Stanley and Wilson 2004;

27 Reeves et al. 2018b; Egerton et al. 2021). However, there have been substantial reductions in the

28 number of platforms in the GOM over the past decade (BOEM 2019; Munnelly et al. 2020).

29 There is debate over whether platforms and similar structures make a substantial contribution to

30 fish stocks (Bohnsack 1989; Claisse et al. 2014; Karnauskas et al. 2017), but platforms certainly

31 have an impact on local ecology and fishing opportunities of coastal communities (Franks 2000;

32 Gallaway et al. 2009; Ajemian et al. 2015). By extension, so do the explosive severance

33 procedures often used to decommission platforms (LGL 2019). Much effort has been devoted at

34 different scales to determining which environmental conditions and platform characteristics

35 affect aspects of platform-associated fish assemblages, but the dynamic nature of the GOM

36 complicates efforts to draw collective inferences.

37   Surveying platforms across the GOM comes with a unique suite of challenges, including

38 accommodating the industrial activities that occur on them and the substantial variation in

39 platform footprint, water depth, and water clarity. Several approaches have been successfully

40 executed, including active acoustic (Stanley and Wilson 1996, 1997; Egerton et al. 2021), hook-

41 and-line (Stanley and Wilson 1991; Rester et al. 2017), optical surveys by various means

42 (Ajemian et al. 2015; Bolser et al. 2020; Wetz et al. 2020), and various combinations of these

43 (Stanley and Wilson 2000, 2004; Reynolds et al. 2018). Prior work has described depth-specific

44 assemblage zonation (Gallaway and Lewbel 1982; Wilson et al. 2006; Ajemian et al. 2015), and

45 seasonal fluctuations in fish density and assemblage composition (Stanley and Wilson 1997;

46 Barker and Cowan 2018; Reynolds et al. 2018). Further, a variety of environmental and habitat-

47 related influences on platform-associated fishes have been identified, including dissolved oxygen
48 concentration (Stanley and Wilson 2004; Reeves et al. 2018b; Egerton et al. 2021), salinity
49 (Gallaway and Lewbel 1982; Munnelly et al. 2019; Bolser et al. 2020), temperature (Gallaway
50 and Lewbel 1982; Stanley and Wilson 1997; Reynolds et al. 2018), artificial light (Barker and
51 Cowan 2018), substrate type, river discharge and *Sargassum* abundance (Munnelly et al. 2020),
52 distance from shore (Bolser et al. 2020), and the number of platforms within 5 km (Bolser et al.
53 2020; Egerton et al. 2021). These studies provide an abundance of valuable information but were
54 conducted at different scales with different methodology. To gain a comprehensive
55 understanding of the relative impact of these factors on a basin-wide scale, it is advantageous to
56 analyze multiple metrics derived from contemporaneously collected data.

57 Optic–acoustic surveys, which typically pair underwater cameras with split-beam
58 echosounders, efficiently provide data on multiple metrics at different resolutions. This approach
59 has increasingly been applied to study fishes around natural and artificial reefs (Lee 2013;
60 Egerton et al. 2018; Demer et al. 2020). Around platforms, optic–acoustic surveys have been
61 applied to describe patterns of distribution, biomass, and density of fishes at different spatial and
62 temporal scales (Stanley and Wilson 2000, 2004; Soldal et al. 2002) and to describe differences
63 in fish assemblages between standing and toppled platforms (Reynolds et al. 2018). optic–
64 acoustic methods are not free of biases, including water clarity for optics, target discrimination
65 and target strength estimation for acoustics (Sawada et al. 1993; Simmonds and MacLennan
66 2008), and exclusion of crypto-benthic fishes for both methods. Nevertheless, optic–acoustic
67 surveys are a relatively rapid, efficient, and robust approach for characterizing water-column fish
68 assemblages (Demer et al. 2020).

69 The present study employs the contemporaneously collected optic and acoustic data of
70 Bolser et al. (2020) and Egerton et al. (2021) to analyze fish assemblages at platforms, and draws
71 collective inferences from these analyses and the published findings of Bolser et al. (2020) and
72 Egerton et al. (2021). We describe our use of optic–acoustic methods to (1) characterize variation
73 in the biomass, size, density, diversity, and richness of water-column fishes at platforms; (2)
74 examine how environmental and platform variables affect fish distribution (water-column and
75 geographic), abundance, biomass, size, density, diversity and richness at platforms in different
76 ways; (3) estimate the average abundance of water-column fishes at platforms; and (4)

77 investigate the impact of scale (i.e., spatial extent and sample size) on our ability to describe

78 environmental and structural effects on fish geographic distributions.

79 **METHODS**

80 **Data Collection**

81   From May–August 2017 and 2018, 114 surveys of 54 platforms were conducted.

82 Platforms were selected via stratified random sampling among depth strata *sensu* Gallaway and

83 Lewbell (1982). Fifty-one platforms were surveyed twice (one optic–acoustic and one optics

84 only) in a single year, and three platforms were surveyed twice in both years (one each of optic–

85 acoustic and optics only in both years). More details on platform selection and characteristics are

86 reported by Bolser et al. (2020) and Egerton et al. (2021).

87   A Simrad EK80 split-beam echosounder with a 120-kHz transducer was pole-mounted to

88 the survey vessel and deployed vertically for hydroacoustic surveys. Hydroacoustic data were

89 collected in a spiral pattern around the platform beginning as close as possible to the platform

90 and ending at approximately 100 m away from it. One additional transect on each side of the

91 structure was also conducted. More details on hydroacoustic data acquisition are reported by

92 Egerton et al. (2021).

93   Following hydroacoustic sampling, the survey vessel was moored to the down-current

94 side of the platform and a YSI EXO sonde was deployed to collect environmental and physical

95 data. The data recorded by the sonde included dissolved oxygen concentration (mg/L),

96 temperature (°C), and salinity (‰). Seafloor depth (m) and platform characteristics were

97 recorded in the field or measured in QGIS (ver. 3.8.1) using data from the Bureau of Ocean and

98 Energy Management (BOEM 2019), with the exception of the distance to natural hard-bottom

99 habitat. To calculate the distance to natural hard-bottom habitat, we generated a 0.008º (2 km x 2

100 km) grid of the presence/absence of rock substrate and reef habitat using data from usSEABED

101 (Buczkowski et al. 2006), ReefBase (http://www.reefbase.org/), and the NOAA Deep Sea Coral

102 Data Portal (https://deepseacoraldata.noaa.gov/). The natural neighbor function in MATLAB

103 (ver. 9.4) was employed to obtain of value of presence/absence of natural hard-bottom habitat for

104 each of the cells of the 0.008° grid. Then, for each of the study platforms, we determined the

105 distance to the nearest natural hard-bottom habitat using the distance function in MATLAB (ver.

106 9.4). The other platform characteristics included: age (years), number of other platforms within 5

107   km, distance from shore (km), and number of legs. More details on sonde measurements and

108   platform characteristics are reported by Bolser et al. (2020) and Egerton et al. (2021).

109   After the sonde sampling, a submersible rotating video (SRV) camera was deployed. The

110   SRV camera was deployed vertically for 6–7 minutes every 10 m of depth approximately 5–6 m

111   away from the platform structure (hereafter, standard drops). A "targeted drop" was conducted in

112   the same manner after hydroacoustic sampling in locations where large schools of fishes were

113   observed on the echosounder. Water clarity was documented for each drop as a visibility score of

114   1–3 (poor to excellent) assigned by an analyst based on their ability to identify fishes (or

115   platform structures if fishes were not observed) at different apparent distances from the camera.

116   Scoring was qualitative due to the lack of direct distance measurements, but it was still possible

117   to discern if fishes were identifiable at only one distance from the camera (i.e., all members of

118   the same species with the same life stage morphology appeared at the same size on the screen;

119   visibility score of 1), at two to three different apparent distances from the camera (visibility score

120   of 2), or more than three different distances from the camera (visibility score of 3). More details

121   on SRV camera deployment and visibility scoring were reported by Bolser et al. (2020).

122   **Data Analysis**

123   Hydroacoustic data were processed using Echoview (ver. 8, Echoview Software)

124   software. Following similar hydroacoustic studies of platform-associated fishes in the GOM, fish

125   densities were derived through echo integral scaling using *in situ* target strength (*TS*)

126   measurements from single targets (Stanley and Wilson 1997, 2000). Target strength

127   measurements that were compromised by multiple echoes were detected using the Nv and M%

128   indices (Sawada et al. 1993; Simmonds and MacLennan 2008) and were masked in Echoview.

129   Fish densities (per volume) derived in this manner were converted to abundance by multiplying

130   by the volume of water investigated out to 100 m from the platform. Thus, reported fish

131   abundance is within 100 m of the platform structure. Mean *TS* (dB re. 1 m^2; a proxy for fish size,

132   hereafter referred to as such) and volumetric backscattering (*Sv*; dB re. 1 m^2; a proxy for fish

133   biomass, hereafter referred to as such) were also extracted from hydroacoustic data, and were

134   first analyzed along with fish density in Egerton et al. (2021). The findings of Egerton et al.

135   (2021) were analyzed further in the present study to place them in context with other metrics

136   derived from contemporaneously collected data so that collective inferences about platform fish

137   assemblages may be drawn. More details on hydroacoustic data processing and the caveats

138   associated with *TS* and *Sv* being used as proxies for fish size and biomass were reported by

139   Egerton et al. (2021).

140   Relative abundances of fish species were estimated from SRV camera data at each 10-m

141   depth layer using the MaxN method (Priede et al. 1994) following similar optical studies of

142   platform-associated fishes in the GOM (Barker and Cowan 2018; Reynolds et al. 2018). Counts

143   commenced at each depth layer after the camera settled and analysts observed the platform

144   structure on a "settled" rotation (typically a 30–45 s waiting period), which typically allowed

145   fishes to resume their normal behavior if it was altered by the camera (Reynolds et al. 2018). In

146   general, fishes were not observed to follow the camera down across multiple depth layers, but we

147   note that it was not possible to completely ensure that all fish observations were unique among

148   depth layers. When targeted drops were conducted in addition to standard drops, the higher of

149   the two MaxN for a given species was taken as the MaxN for that depth layer.

150   Hydroacoustic estimates of fish abundance in each 10-m depth layer were apportioned

151   according to the relative abundance (proportion) of each species in each 10-m depth layer. The

152   resultant species abundance at each depth layer was summed across depth layers to provide an

153   estimate of the abundance of each species at each study platform. Given the influence of water

154   clarity on estimates of relative abundance measured by optical gears, we present two estimates of

155   the average optic–acoustic abundance of species: one from the full dataset, and one from only

156   sites with visibility scores greater than 2.0/3.0 (the reduced dataset). Cryptic, strongly reef-

157   associated species, and megafauna (Supplemental Appendix 3) were excluded from the analyses

158   due to either the low likelihood of detection by the echosounder, given their close proximity to

159   the platform structure and/or high inconsistency in detection by the SRV camera. Thus, the

160   present study only considered common platform-associated species that were typically found in

161   the water column at distances $> \sim 1$ m away from the platform structure.

162   MaxN counts were reduced to encounter/non-encounter at each site to analyze species

163   geographic distribution, species richness and Shannon–Wiener diversity (hereafter, diversity;

164   Shannon 1948). For representing data in figures of diversity and richness at sites that were

165   surveyed more than once, a species was recorded as "encountered" if it was observed in any of

166   the visits and "not encountered" if it was never observed at the site. Site visits were treated

167   separately in the dataset used to analyze these metrics statistically.

168   **Statistical Analysis**

169   All statistical analyses were conducted in R Studio (ver. 3.6.1). We fit generalized

170   additive mixed models (GAMMs) to examine the influence of environmental conditions and

171   platform characteristics on species richness and diversity. Based on data distribution, we fit

172   Gaussian (for richness) and Quasi-Poisson (for diversity) GAMMs with identity (for richness)

173   and log (for diversity) link functions using the "mgcv" (ver. 1.8-28) R package. Prior to

174   modelling, correlations between potential predictors were examined, and of the predictors with a

175   correlation coefficient greater than 0.7 in absolute value, the predictor with the lowest mean

176   correlation with diversity and richness was excluded from the analysis (Grüss et al. 2020).

177   Predictors that were not correlated with one another or with eastings or northings above an

178   absolute value of 0.7 were included as smoothed predictors in the initial models (Grüss et al.

179   2020). Non-significant predictors were later excluded from the GAMMs, which were re-fit until

180   only significant predictors remained in the final model following the approach described by

181   Bolser et al. (2020) and Egerton et al. (2021). Visibility score, site, and survey team were

182   included as random effects in these models, as water clarity affects fish detectability, sites were

183   visited multiple times, and two survey teams collected data. A tensor term between eastings and

184   northings was also included as a fixed effect to account for spatial autocorrelation in the data.

185   The GAMMs were evaluated using an approach in which Spearman correlation coefficients

186   (Spearman ρ) between GAMM predictions and observed data were calculated and tested to be

187   significantly different from zero (Egerton et al. 2021; Grüss et al. 2021).

188   We also fit single-predictor negative binomial Generalized Additive Models (GAMs)

189   with a log link function to understand the influence of environmental conditions and platform

190   characteristics on the abundance of three federally managed platform-associated species: Greater

191   Amberjack *Seriola dumerili*, Red Snapper *Lutjanus campechanus*, and Vermilion Snapper

192   *Rhomboplites aurorubens*. We fit single-predictor GAMs instead of multiple-predictor

193   GAM(M)s to avoid overfitting as the models were fit only to data from the reduced dataset

194   (Figure 1). Models fit to the entire dataset were also explored (see supplementary material). We

195   considered the same predictors in these models as in the GAMMs of species richness and

196   diversity, and the GAMMS fit in Bolser et al. (2020) and Egerton et al. (2021)—excluding

197   turbidity (Supplemental Table 4).

198   In the same manner as the GAMs of abundance, single-predictor binomial GAMs with

199   logit link functions were fit to encounter/non-encounter data of Greater Amberjack, Red

200   Snapper, and Vermilion Snapper from the reduced dataset to investigate influences on their

201   geographic distributions at the same scale as the abundance. Predictors included in this analysis

202   were the same as above (Supplemental Table 4). A similar procedure was used to study the

203   geographic distributions of these species using the full dataset by Bolser et al. (2020), but the

204   analysis in the present study was conducted to investigate the role of scale in our ability to

205   describe the effects of environmental conditions and platform characteristics on fish geographic

206   distributions.

207   Wisconsin–standardized encounter/non-encounter data for each species were analyzed by

208   non-metric multi-dimensional scaling (NMDS) using Jaccard distances through the "metaMDS"

209   function in the "vegan" (ver. 2.5-6) R package to examine variation in assemblage. A smoothed

210   surface for each of the significant predictors in diversity and richness GAMMs was generated in

211   the NMDS space using the "ordisurf" function in vegan for observation of the interplay between

212   gradients in these variables and variation in assemblage. A smoothed surface for seafloor depth

213   was also generated and plotted given the findings of prior work linking variation in assemblage

214   with seafloor depth (e.g., Gallaway and Lewbel 1982; Wilson et al. 2006; Ajemian et al. 2015).

215   The ordisurf function fits a GAM to generate the smoothed surface. We modified the base

216   settings of ordisurf to fit GAMs with penalized thin plate regression splines (fx = T, bs = "ts"),

217   and generated plots by modifying code from the "ggordiplots" R package. Species that were

218   significantly associated with the spread of NMDS points (i.e., their encounter/non-encounter was

219   associated with differences in the position of sites in the NMDS space) were identified using the

220   "envfit" permutation function in vegan, and their corresponding vectors were plotted. These

221   vectors represented the directionality and strength of the relationship.

222   **RESULTS**

223   **Average Abundance of Species**

224   Species abundances were highly variable between sites, as evidenced by standard

225   deviations of abundance, which exceeded mean abundances for every species except Red

226   Snapper (Table 1). Percentage differences between abundance estimates from sites with good

227   water clarity (the reduced dataset, n = 19) and all sites (n = 54) ranged from 19.0 – 350.7%

228   (mean = 65.6%) for the 15 most abundant species in our dataset. Abundance estimates for all are

229   reported in Supplemental Table 2. Though study platforms were distributed widely from

230 nearshore to far offshore areas off the coasts of Texas through Alabama, platforms with good
231 water clarity were generally found offshore in the western GOM (Figure 1).

232 **Diversity and Richness**

233 Species diversity and species richness varied spatially, with the lowest richness and
234 diversity found on platforms nearest to the Mississippi River outflow, and the highest generally
235 at offshore platforms in the western GOM (Figures 2, 3). When these results were considered
236 along with the findings of Egerton et al. (2021) on fish biomass and size proxies (see Egerton et
237 al. 2021 for details) and density from acoustic data collected at the same site visit, we observed
238 that the sites with the highest values of diversity and richness also tended to exhibit high fish
239 biomass and density values (Figures 2, 3).

240 The GAMMs fit to species richness and diversity data suggested that salinity and distance
241 from shore explained a large proportion of the variance in diversity (Figure 4; adjusted-R^2: 0.50,
242 CI: 0.37–0.64) and richness (Figure 5; adjusted-R^2: 0.45, CI: 0.32–0.59). The marginal effect of
243 salinity on diversity showed a positive relationship with salinity from approximately 26 to 33 ‰,
244 after which the relationship was slightly negative, though the effect was positive from
245 approximately 32 to 37 ‰ (Figure 4). Similarly, the marginal effect of distance from shore on
246 diversity showed a positive relationship with distance from shore until approximately 90 km
247 from shore, after which the relationship was negative, though the effect was positive at distances
248 approximately 50 km from shore and beyond (Figure 5). The marginal effects of salinity and
249 distance from shore on richness showed similar patterns (Figure 5). Distance from shore
250 explained the majority of the variance in diversity (Figure 4) and species richness (Figure 5)
251 compared to salinity, eastings, and northings. The Spearman ρ of the richness GAMM was 0.62
252 (CI: 0.51–0.77, $p < 0.0001$) and the Spearman ρ of the diversity GAMM was 0.70 (CI: 0.61–
253 0.84, $p < 0.0001$), so both GAMMs passed the evaluation test and could be employed for
254 statistical inferences. These results, when considered along with the results of Bolser et al.
255 (2020) and Egerton et al. (2021), suggested that variables related to freshwater inflow and meso-
256 scale circulation patterns affected the greatest number of aspects of platform-associated fish
257 assemblages (Table 2).

258 **Effects on the Distribution and Abundance of Greater Amberjack, Red Snapper, and**
259 **Vermilion Snapper**

260 The geographic distributions of Greater Amberjack, Red Snapper, and Vermilion Snapper
261 were not influenced by any predictors included in GAMs fit to the reduced dataset. Similarly, the
262 abundances of Red Snapper and Vermilion Snapper were not influenced by any of the predictors
263 included in GAMs fit to the reduced dataset, while the marginal effect of distance from shore on
264 the abundance of Greater Amberjack had a positive relationship with distance from shore ($p <$
265 0.001; EDF = 1.07; adjusted-R^2 = 0.26; Table 3; Supplemental Figure 1). Differences between
266 the geographic distribution results of the present study and those of Bolser et al. (2020)
267 suggested that spatial scale likely affected our ability to describe the effects variables on
268 geographic distribution and abundance (Table 3).

269 **Non-Metric Multidimensional Scaling Analysis of Assemblage**

270 Distinct assemblage groupings were not observed in the NMDS space (Figure 6). Instead,
271 platform fish assemblages varied gradually along gradients of distance from shore, salinity, and
272 depth (Figure 6). Variation in assemblage was associated with the encounter/non-encounter of
273 the following species: Almaco Jack *Seriola rivoliana* ($p = 0.001$, R^2 = 0.38), Atlantic Bumper
274 *Chloroscombrus chrysurus* ($p = 0.001$, R^2 = 0.36), Atlantic Spadefish *Chaetodipterus faber* ($p =$
275 0.001, R^2 = 0.34), Bermuda Chub *Kyphosus sectatrix* ($p = 0.001$, R^2 = 0.55), Cobia
276 *Rachycentron canadum* ($p = 0.001$, R^2 = 0.21), Crevalle Jack (*Caranx hippos* ($p = 0.001$, R^2 =
277 0.30), Gray Triggerfish *Balistes capriscus* ($p = 0.33$, R^2 = 0.12), Great Barracuda *Sphyraena*
278 *barracuda* ($p = 0.001$, R^2 = 0.50), Greater Amberjack ($p = 0.001$, R^2 = 0.56), Ocean Triggerfish
279 *Canthidermis sufflamen* ($p = 0.003$, R^2 = 0.23), Rainbow Runner *Elagatis bipinnulata* ($p = 0.01$,
280 R^2 = 0.15), Red Snapper ($p = 0.002$, R^2 = 0.28), Sheepshead *Archosargus probatocephalus* ($p =$
281 0.005, R^2 = 0.20), and Vermilion Snapper ($p = 0.003$, R^2 = 0.20; Figure 6).

282 **DISCUSSION**

283 Our analysis of contemporaneously collected optic and acoustic data allowed us to
284 explore the effects of environmental conditions and platform characteristics on many different
285 aspects of platform-associated fish assemblages. Numerous species may be encountered across a
286 relatively wide range of conditions at platforms (Bolser et al. 2020), but environmental
287 conditions and platform characteristics affected fish assemblage metrics nonetheless.
288 Environmental conditions related to freshwater inflow and meso-scale circulation patterns (e.g.,
289 salinity, temperature, dissolved oxygen concentration) affected more metrics than platform
290 characteristics (e.g., distance from shore, number of platforms within 5 km, seafloor depth; Table

291 2). However, gradual variation in assemblage was observed along gradients of both types of
292 variables in the NMDS space (Figure 6).

293   The gradients in salinity, temperature, and dissolved oxygen—the variables that affected
294 the highest numbers of our metrics—observed in this study can mostly be attributed to
295 freshwater inflow from the Mississippi and Atchafalaya rivers and Loop Current-driven
296 circulation patterns. Accordingly, our findings add to existing knowledge of how these meso-
297 scale features affect ecosystem and community dynamics in the GOM (Table 2; e.g., Gallaway
298 1981; Dagg and Breed 2003; Hetland and DiMarco 2008). The effects of salinity, which
299 influenced all of our metrics, on platform-associated fish assemblages are likely indirect. In other
300 words, it is unlikely that the range of salinities we encountered was physiologically stressful to
301 the fishes in our study. Instead, salinity is negatively associated with productivity (Kim et al.
302 2020) and tracks Caribbean water masses containing diverse groups of fish larvae in offshore
303 areas of the GOM (Gallaway 1981; Gallaway and Lewbell 1982). Temperature is likely similar
304 to salinity in acting indirectly and tracing water masses (Mamayev 2010). Thus, the effects of
305 salinity and temperature on platform-associated fishes likely reflect the proximate effect of
306 productivity and other aspects of water masses (e.g., larval transport).

307   Platform characteristics affected fewer metrics than environmental conditions, but still
308 influenced species richness, diversity, and the distributions of a small number of species (Table
309 2; Bolser et al. 2020). While distance from shore and the number of platforms near the study
310 platform had not been examined explicitly by other authors in other studies of platform fish
311 assemblages to our knowledge, prior work suggested that assemblages varied by seafloor depth
312 at platforms (Gallaway and Lewbel 1982; Wilson et al. 2006; Ajemian et al. 2015). Patterns
313 observed in the NMDS space (Figure 6) generally support these findings, although seafloor depth
314 was not a significant predictor in any models of assemblage metrics or species geographic
315 distributions (Table 2; Bolser et al. 2020), and we did not observe distinct assemblage groupings
316 (Figure 6). Seafloor depth has been useful for designating sampling strata in past studies of
317 platform-associated fish assemblages, but our results suggest that researchers should also
318 consider distance from shore when planning their sampling schemes.

319   We found that species richness and diversity often increased with increasing distance
320 from shore (Figures 2–5). Conditions at offshore areas are generally thought to be more stable
321 than at nearshore areas, which likely facilitates the colonization and persistence of corals and

322   small reef fishes that are transported to platforms by meso-scale circulation patterns (Gallaway

323   1981; Kolian et al. 2017; Kolian and Sammarco 2019). These types of organisms were not

324   considered in the present study, but their presence at offshore platforms may have affected

325   water-column fishes and contributed to the trends we described indirectly. Diverse fish

326   assemblages also exist at natural hard-bottom habitats in offshore areas, and it is likely that some

327   species observed at platforms interact with nearby natural habitats (Cowan and Rose 2016).

328   However, we did not find that the distance to natural hard-bottom habitat had an influence on the

329   richness or diversity of water-column fish assemblages at platforms. In addition to stable

330   conditions and favorable circulation patterns, the lower fishing pressure that offshore platforms

331   likely experience compared to nearshore platforms could have also contributed to higher richness

332   and diversity in this area, and at platforms further from shore in general (Pauly et al. 2002)

333   (Figures 2–5).

334   The most species-rich and diverse platforms tended to have the greatest fish biomasses

335   and densities (Figures 2, 3). This result agrees with prior work, which documented a positive

336   relationship between abundance and richness in reef habitats globally (Edgar et al. 2017), but

337   occurs despite generally opposing effects of salinity on richness and diversity (positive

338   relationship until 33–34 ‰) and fish biomass and density (negative relationship; Table 2). As

339   identified above, salinity and productivity are closely related in the Gulf of Mexico (Kim et al.

340   2020), and many of the platforms that exhibited high levels of fish biomass, density, diversity,

341   and richness were located offshore of the Atchafalaya River. The Atchafalaya River has an

342   important influence on the productivity and physiochemical characteristics of the region's waters

343   (Hetland and DiMarco 2008; DiMarco et al. 2010; Kim et al. 2020). The fish assemblages at

344   platforms in this "hotspot" may be close enough to the Atchafalaya River outflow to benefit from

345   freshwater inflow-derived productivity, yet may be far enough offshore that local effects of

346   hypoxia are not substantial. Freshwater inflow-derived productivity may outweigh local effects

347   of hypoxia in the wider region (de Mutsert et al. 2016), but potentially not at the platforms

348   nearest to the outlet of the Mississippi River, which we observed to have low fish biomass,

349   density, diversity, and richness (Figures 2, 3). These platforms may also fall within a "Brown

350   Zone" where high sediment loading stifles primary productivity (Rowe and Chapman 2002; Kim

351   et al. 2020). In general, however, the comparatively higher primary productivity at nearshore

352   platforms supports more productive fouling communities, which in turn may support a variety of

353   grazing species (e.g., Sheepshead, Gray Triggerfish, Black Drum *Pogonias cromis*; Reeves et al.

354   2018a). Despite this, the conditions at offshore platforms appear to support more diverse, rich,

355   and abundant water-column fish assemblages.

356   Importantly, platforms further from shore tended to have the best water clarity. Prior

357   studies have found that water clarity and associated variables (e.g., turbidity) are important

358   drivers of variation in different aspects of fish assemblages (e.g., Cyrus and Blaber 1992).

359   However, we did not include water clarity as a fixed environmental covariate having a direct

360   effect on the dependent variable in our models fit to the full dataset, but rather as a random

361   nuisance factor (visibility score) to account for the effect of water clarity on species detection

362   with optical methods. Given the greater influence of water clarity on relative abundance

363   compared to encounter/non-encounter data, we also presented abundance analyses conducted on

364   only the reduced dataset (but see the supplementary material for exploratory analyses on the full

365   dataset) and presented estimates of abundance for both the full and reduced datasets for

366   comparison. Non-optical methods are best suited for documenting the direct effects of water

367   clarity and associated variables on fish assemblages, and the acoustic study of Egerton et al.

368   (2021) at our study platforms indicated that turbidity did not affect platform fish density,

369   biomass, and size at a wide spatial scale. Still, water clarity could affect the distribution and

370   abundance of certain platform-associated species, and this should be investigated in future non-

371   optical studies.

372   In both the full and reduced datatsets, relatively small pelagic planktivores (e.g., Atlantic

373   Bumper, Blue Runner *C. crysos*) dominated the platform-associated fish assemblage, followed

374   by larger piscivorous species such as Red Snapper and Greater Amberjack (Table 1).

375   Abundances were highly variable for all species (Table 1), though in different ways. Species

376   such as Red Snapper and Blue Runner were encountered at most study platforms (Bolser et al.

377   2020; Supplementary Table 3) but with varying abundances. Others, like Atlantic Bumper or

378   Vermilion Snapper, were encountered at a small number of platforms (Bolser et al. 2020;

379   Supplementary Table 3), but were highly abundant when they were encountered. Still others

380   such as the Great Barracuda and Gray Snapper *L. griseus* were encountered often (Bolser et al.

381   2020; Supplementary Table 3), but at consistently lower numbers than many other common

382   species.

383   It was not possible to develop models of species abundance for the full dataset that we
384   were confident about, and the reduced dataset containing only sites with good water clarity
385   covered a spatial scale that was likely too small to identify variables that affect species
386   abundance. The influence of spatial scale on our ability to describe effects was illustrated by the
387   comparison of geographic distribution analyses between the present study, which employed the
388   reduced dataset, and the study of Bolser et al. (2020), which employed the full dataset. We did
389   not detect any effect of environmental conditions or platform characteristics on the geographic
390   distributions of Red Snapper, Vermilion Snapper, and Greater Amberjack, which differed from
391   the findings of Bolser et al. (2020; Table 3). Since Bolser et al. (2020) accounted for water
392   clarity in their models, the differences between the study of Bolser et al. (2020) and the present
393   study may be explained by spatial scale. Our examination of the abundance of those species in
394   the reduced dataset solely identified the influence of distance from shore on Greater Amberjack
395   abundance, and based on our comparison of geographic distribution analyses, we conclude that
396   our results were impacted by the restricted spatial scale of the reduced dataset (Table 3). Our
397   findings illustrate the problem of extending the conclusions of small-scale studies to wide areas
398   (Levin 1992). Scale-dependence of effects and ability to detect them likely explain a large
399   number of the discrepancies in the literature regarding the effects of different variables on
400   platform-associated fishes in the GOM.
401   The substantial variation in abundance observed for common platform-associated species
402   is more likely explained by variable movement patterns and complex ecological dynamics than
403   simple variation in platform characteristics and environmental conditions at the spatial scale of
404   the reduced dataset (Kraft et al. 2015). For example, while some platform-associated species
405   exhibit homing behavior and relatively high residency on platforms (e.g., Red Snapper;
406   Gallaway et al. 2009; Blue Runner; Brown et al. 2010), they may also travel long distances and
407   spend long periods of time away from the sites at which they were tagged (e.g., Red Snapper,
408   Gallaway et al. 2009). Other species simply associate with platforms opportunistically (Franks
409   2000). Considering the behavior of mobile species and the highly variable abundances we
410   observed, and that relatively few species' distributions were influenced by environmental
411   conditions and platform characteristics (Bolser et al. 2020), we conclude that observing a large
412   number of a given species during one visit to a platform does not guarantee the same thing
413   during another visit. This is important to consider when interpreting our results, as despite

414 repeated visits to each site, our sampling was closer to a "snapshot" than a continuous record of
415 variation of fish assemblages at platforms. Definitively uncovering the sources of variation in
416 fish abundance at platforms on a basin-wide scale will require relatively long-term observations.

417 **ACKNOWLEDGMENTS**

432 **REFERENCES**

433 Ajemian, M. J., J. J. Wetz, B. Shipley-Lozano, J. D. Shively, and G. W. Stunz. 2015. An analysis
434   of artificial reef fish community structure along the northwestern Gulf of Mexico shelf:
435   potential impacts of "Rigs-to-Reefs" programs. PLOS ONE 10(5):e0126354.
436 Barker, V. A., and J. H. Cowan. 2018. The effect of artificial light on the community structure of
437   reef-associated fishes at oil and gas platforms in the northern Gulf of Mexico.
438   Environmental Biology of Fishes 101(1):153–166.
439 Bohnsack, J. A. 1989. Are high densities of fishes at artificial reefs the result of habitat limitation
440   or behavioral preference? Bulletin of Marine Science 44(2):631–645.
441 Bolser, D. G., J. P. Egerton, A. Grüss, T. Loughran, T. Beyea, K. McCain, and B. E. Erisman.
442   2020. Environmental and structural drivers of fish distributions among petroleum
443   platforms across the U.S. Gulf of Mexico. Marine and Coastal Fisheries 12(2):142–163.

444 Brown, H., M. C. Benfield, S. F. Keenan, and S. P. Powers. 2010. Movement patterns and home
445   ranges of a pelagic carangid fish, *Caranx crysos*, around a petroleum platform complex.
446   Marine Ecology Progress Series 403:205–218.

447 Buczkowski, J., J. A. Reid, C. J. Jenkins, J. M. Reid, S. J. Williams, J. G. Flocks, P. P. Leahy, A.
448   Director, and C. J. Jenkins. 2006. U.S. Geological Survey.

449 Claisse, J. T., D. J. Pondella, M. Love, L. A. Zahn, C. M. Williams, J. P. Williams, and A. S.
450   Bull. 2014. Oil platforms off California are among the most productive marine fish
451   habitats globally. Proceedings of the National Academy of Sciences 111(43):15462–
452   15467.

453 Cowan, J. H., and K. A. Rose. 2016. Oil and gas platforms in the Gulf of Mexico: their
454   relationship to fish and fisheries. Fisheries and aquaculture in the modern world.
455   IntechOpen, London.

456 Cyrus, D. P., and S. J. M. Blaber. 1992. Turbidity and salinity in a tropical northern Australian
457   estuary and their influence on fish distribution. Estuarine Coastal and Shelf Science
458   35:545–563.

459 Dagg, M. J., and G. A. Breed. 2003. Biological effects of Mississippi River nitrogen on the
460   northern gulf of Mexico—a review and synthesis. Journal of Marine Systems 43(3):133–
461   152.

462 Demer, D. A., W. L. Michaels, T. Algrøy, L. N. Andersen, O. Abril-Howard, B. Binder, D.
463   Bolser, R. Caillouet, M. D. Campbell, S. Cambronero-Solano, E. Castro-Gonzalez, J.
464   Condiotty, J. Egerton, V. E. González-Maynez, T. Jarvis, M. Mayorga-Martínez, J.
465   Paramo-Granados, C. Roa, A. Rojas-Archbold, J. Sintura-Arango, J. C. Taylor, C. H.
466   Thompson, and H. Villalobos. 2020. Integrated optic–acoustic studies of reef fish: report
467   of the 2018 GCFI Field Study and Workshop. NOAA National Marine Fisheries Service
468   Report. Available: https://bit.ly/3i8lPvd.

469 DiMarco, S. F., P. Chapman, N. Walker, and R. D. Hetland. 2010. Does local topography control
470   hypoxia on the eastern Texas–Louisiana shelf? Journal of Marine Systems 80(1):25–35.

471 Edgar, G. J., T. J. Alexander, J. S. Lefcheck, A. E. Bates, S. J. Kininmonth, R. J. Thomson, J. E.
472   Duffy, M. J. Costello, and R. D. Stuart-Smith. 2017. Abundance and local-scale
473   processes contribute to multi-phyla gradients in global marine diversity. Science
474   Advances 3(10):e1700419.

475   Egerton, J. P., A. F. Johnson, J. Turner, L. LeVay, I. Mascareñas-Osorio, and O. Aburto-
476   Oropeza. 2018. Hydroacoustics as a tool to examine the effects of Marine Protected
477   Areas and habitat type on marine fish communities. Scientific Reports 8:47.

478   Egerton, J. P., D. G. Bolser, A. Grüss, and B. E. Erisman. 2021. Understanding patterns of fish
479   backscatter, size and density around petroleum platforms of the U.S. Gulf of Mexico
480   using hydroacoustic data. Fisheries Research 233:105752.

481   Franks, J. 2000. A review: pelagic fishes at petroleum platforms in the northern Gulf of Mexico;
482   diversity, interrelationships, and perspective. Available: https://bit.ly/3hAhlOV.

483   Gallaway, B. J. 1981. An ecosystem analysis of oil and gas development on the Texas-Louisiana
484   Continental Shelf. U.S. Department of the Interior, Bureau of Land Management, Fish
485   and Wildlife Service. Available: https://bit.ly/3ySTbFf.

486   Gallaway, B. J., and G. S. Lewbel. 1982. The ecology of petroleum platforms in the
487   northwestern Gulf of Mexico: a community profile. U.S. Department of the Interior,
488   Bureau of Land Management, Fish and Wildlife Service. Available:
489   https://bit.ly/3kiHcwH.

490   Gallaway, B. J., S. T. Szedlmayer, and W. J. Gazey. 2009. A life history review for Red Snapper
491   in the Gulf of Mexico with an evaluation of the importance of offshore petroleum
492   platforms and other artificial reefs. Reviews in Fisheries Science 17(1):48–67.

493   Grüss, A., M. Drexler, and C. H. Ainsworth. 2014. Using delta generalized additive models to
494   produce distribution maps for spatially explicit ecosystem models. Fisheries Research
495   159:11–24.

496   Grüss, A., J. L. Pirtle, J. T. Thorson, M. R. Lindeberg, A. D. Neff, S. G. Lewis, and T. E.
497   Essington. 2021. Modeling nearshore fish habitats using Alaska as a regional case study.
498   Fisheries Research 238:105905.

499   Grüss, A., K. A. Rose, D. Justić, and L. Wang. 2020. Making the most of available monitoring
500   data: a grid-summarization method to allow for the combined use of monitoring data
501   collected at random and fixed sampling stations. Fisheries Research 229:105623.

502   Hetland, R. D., and S. F. DiMarco. 2008. How does the character of oxygen demand control the
503   structure of hypoxia on the Texas–Louisiana continental shelf? Journal of Marine
504   Systems 70(1):49–62.

505   Karnauskas, M., J. F. W. III, M. D. Campbell, A. G. Pollack, J. M. Drymon, and S. Powers.

506   2017. Red Snapper distribution on natural habitats and artificial structures in the northern

507   Gulf of Mexico. Marine and Coastal Fisheries 9(1):50–67.

508   Kim, J., P. Chapman, G. Rowe, and S. F. DiMarco. 2020. Categorizing zonal productivity on the

509   continental shelf with nutrient-salinity ratios. Journal of Marine Systems 206:103336.

510   Kolian, S. R., and P. W. Sammarco. 2019. Densities of reef-associated fish and corals on

511   offshore platforms in the Gulf of Mexico. Bulletin of Marine Science 95(3):393–407.

512   Kolian, S. R., P. W. Sammarco, and S. A. Porter. 2017. Abundance of Corals on Offshore Oil

513   and Gas Platforms in the Gulf of Mexico. Environmental Management 60(2):357–366.

514   Kraft, N. J. B., P. B. Adler, O. Godoy, E. C. James, S. Fuller, and J. M. Levine. 2015.

515   Community assembly, coexistence and the environmental filtering metaphor. Functional

516   Ecology 29(5):592–599.

517   Lee, D.-J. 2013. Monitoring of fish aggregations responding to artificial reefs using a split-beam

518   echo sounder, side-scan sonar, and an underwater CCTV camera system at Suyeong Man,

519   Busan, Korea. Korean Journal of Fisheries and Aquatic Sciences 46(3):266–272.

520   Levin, S. A. 1992. The problem of pattern and scale in ecology: the Robert H. MacArthur Award

521   lecture. Ecology 73(6):1943–1967.

522   LGL Ecological Research Associates. 2019. Characterization of fish assemblages associated with

523   offshore oil and gas platforms in the Gulf of Mexico. Report for Contract No.

524   M16PC00005. 10.13140/RG.2.2.28322.25282.

525   Mamayev, O. I. 2010. Temperature-salinity analysis of world ocean waters. Elsevier,

526   Amsterdam.

527   Munnelly, R. T., D. B. Reeves, E. J. Chesney, D. M. Baltz, and B. D. Marx. 2019. Habitat

528   suitability for oil and gas platform-associated fishes in Louisiana's nearshore waters.

529   Marine Ecology Progress Series 608:199–219.

530   Munnelly, R. T., D. B. Reeves, E. J. Chesney, and D. M. Baltz. 2020. Spatial and temporal

531   influences of nearshore hydrography on fish assemblages associated with energy

532   platforms in the northern Gulf of Mexico. Estuaries and Coasts. Available:

533   https://bit.ly/3wIYRjW.

534   de Mutsert, K., J. Steenbeek, K. Lewis, J. Buszowski, J. H. Cowan, and V. Christensen. 2016.
535   Exploring effects of hypoxia on fish and fisheries in the northern Gulf of Mexico using a
536   dynamic spatially explicit ecosystem model. Ecological Modelling 331:142–150.

537   Pauly, D., V. Christensen, S. Guénette, T. J. Pitcher, U. R. Sumaila, C. J. Walters, R. Watson,
538   and D. Zeller. 2002. Towards sustainability in world fisheries. Nature 418(6898):689–
539   695.

540   Priede, I. G., P. M. Bagley, A. Smith, S. Creasey, and N. R. Merrett. 1994. Scavenging deep
541   demersal fishes of the Porcupine Seabight, north-east Atlantic: observations by baited
542   camera, trap and trawl. Journal of the Marine Biological Association of the United
543   Kingdom 74(3):481–498. Cambridge University Press.

544   Reeves, D. B., E. J. Chesney, R. T. Munnelly, and D. M. Baltz. 2018a. Barnacle settlement and
545   growth at oil and gas platforms in the northern Gulf of Mexico. Marine Ecology Progress
546   Series 590:131–143.

547   Reeves, D. B., E. J. Chesney, R. T. Munnelly, D. M. Baltz, and B. D. Marx. 2018b. Abundance
548   and distribution of reef-associated fishes around small oil and gas platforms in the
549   northern Gulf of Mexico's hypoxic zone. Estuaries and Coasts 41(7):1835–1847.

550   Reynolds, E. M., J. H. Cowan, K. A. Lewis, and K. A. Simonsen. 2018. Method for estimating
551   relative abundance and species composition around oil and gas platforms in the northern
552   Gulf of Mexico, U.S.A. Fisheries Research 201:44–55.

553   Rowe, G. T., and P. Chapman. 2002. Continental shelf hypoxia: some nagging questions. Gulf of
554   Mexico Science 20(2). Available: https://bit.ly/36zEhI4.

555   Sawada, K., M. Furusawa, and N. J. Williamson. 1993. Conditions for the precise measurement
556   of fish target strength *in situ*. The Journal of the Marine Acoustics Society of Japan
557   20(2):73–79.

558   Shannon, C. E. 1948. A mathematical theory of communication. The Bell System Technical
559   Journal 27(3):379–423.

560   Simmonds, J., and D. N. MacLennan. 2008. Fisheries acoustics: theory and practice. John Wiley
561   and Sons, Hoboken, New Jersey.

562   Soldal, A. V., I. Svellingen, T. Jørgensen, and S. Løkkeborg. 2002. Rigs-to-reefs in the North
563   Sea: hydroacoustic quantification of fish in the vicinity of a "semi-cold" platform. ICES
564   Journal of Marine Science 59(suppl):S281–S287.

565   Stanley, D. R., and C. A. Wilson. 1991. Factors affecting the abundance of selected fishes near
566   oil and gas platforms in the northern Gulf of Mexico. Fishery Bulletin; (United States)
567   89:1. Available: https://bit.ly/3eaWcJ1.

568   Stanley, D. R., and C. A. Wilson. 1996. Abundance of fishes associated with a petroleum
569   platform as measured with dual-beam hydroacoustics. ICES Journal of Marine Science
570   53(2):473–475.

571   Stanley, D. R., and C. A. Wilson. 1997. Seasonal and spatial variation in the abundance and size
572   distribution of fishes associated with a petroleum platform in the northern Gulf of
573   Mexico. Canadian Journal of Fisheries and Aquatic Sciences 54(5):1166–1176.

574   Stanley, D. R., and C. A. Wilson. 2000. Variation in the density and species composition of
575   fishes associated with three petroleum platforms using dual beam hydroacoustics.
576   Fisheries Research 47(2):161–172.

577   Stanley, D. R., and C. A. Wilson. 2004. Effect of hypoxia on the distribution of fishes associated
578   with a petroleum platform off coastal Louisiana. North American Journal of Fisheries
579   Management 24(2):662–671.
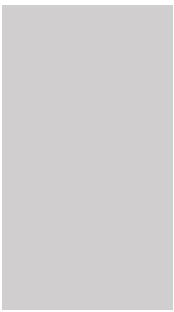
580   Wetz, J. J., M. J. Ajemian, B. Shipley, and G. W. Stunz. 2020. An assessment of two visual
581   survey methods for documenting fish community structure on artificial platform reefs in
582   the Gulf of Mexico. Fisheries Research 225:105492.

583   Wilson, C.A., M. W. Miller, Y. C. Allen, K. M. Boswell, and D. L. Nieland. 2006. Effects of
584   depth, location, and habitat type on relative abundance and species composition of fishes
585   associated with petroleum platforms and the Sonnier Bank in the northern Gulf of
586   Mexico. U.S. Dept. of the Interior, Minerals Management Service, Gulf of Mexico OCS
587   Region, New Orleans. OCS Study MMS 2006-037.

588

Species	Average Abundance from Sites with Visibility Scores > 2.0/3.0 (Standard Deviation)	Average Abundance from All Sites (Standard Deviation)	Percentage Difference in Average Abundance
Atlantic Bumper Chloroscombrus chrysurus	11,778 (22,662)	4,749 (14,161)	59.68
Blue Runner Caranx crysos	6,869 (8,750)	8,959 (14,056)	30.44
Bermuda Chub Kyphosus sectatrix	4,194 (8,839)	1,673 (5,446)	60.10
Red Snapper Lutjanus campechanus	3,871 (2,971)	2,347 (2,489)	39.37
Greater Amberjack Seriola dumerili	2,243 (7,308)	1,566 (5,965)	30.21
Crevalle Jack C. hippos	2,121 (6,831)	1,484 (5,702)	30.03
Vermilion Snapper Rhomboplites aurorubens	1,190 (2,169)	964 (3,184)	19.00
Atlantic Moonfish Selene setapinnis	864 (3,638)	304 (2,121)	64.83
Atlantic Spadefish Chaetodipterus faber	751 (1,391)	3,383 (16,124)	350.67
Guachanche Barracuda Sphyraena guachancho	660 (2,330)	224 (1,370)	66.07
Gray Snapper L. griseus	655 (1,313)	516 (1,253)	21.24
Horse-Eye Jack C. latus	576 (1,913)	217 (1,130)	62.30
Rainbow Runner Elagatis bipinnulata	553 (2,296)	270 (1,410)	51.21
Almaco Jack S. rivoliana	289 (688)	383 (1,840)	32.39
Bluefish Pomatomus saltatrix	192 (837)	65 (488)	66.07

Table 1. Average and standard deviation of optic–acoustic abundance within 100 m of platform structure for the 15 most abundant species in our dataset. The average and standard deviation of abundance of fishes is presented for study sites with good water column visibility (average visibility scores > 2.0/3.0, n = 19), and for all study sites (n = 54), along with the percentage difference in abundance estimates derived from these datasets.

Parameter	Species Richness (optic)	Shannon-Weiner Diversity (optic)	Species Distribution – geographic (optic)	Species Distribution – depth (optic)	Fish Biomass (acoustic)	Fish Density (acoustic)	Fish Size (acoustic)
Salinity (psu)	D/A	D/A	+/D/A (2 spp.)	+ (2 spp.)	-	-	P
Temperature (°C)				+/D/A (5 spp.)	+	D/A	+
Dissolved Oxygen Concentration (mg/L)			+ (1 spp.)	+ (1 spp.)		+	
Distance from Shore (km)	D/A	D/A	+/D/A (3 spp.)				
Number of Platforms within 5 km			- (2 spp.)		-		
Seafloor Depth (m)				- (1 spp.)			

Species	Parameter	Negative Binomial GAM (abundance)	Binomial GAM (encounter/non-encounter)	Binomial GAMM (encounter/non-encounter; Bolser et al. 2020)
Greater Amberjack Seriola dumerili	Distance from Shore (km)	+		D/A
Red Snapper Lutjanus campechanus	Dissolved Oxygen Concentration (mg/L)			+
	Salinity (psu)			D/A
Vermilion Snapper Rhomboplites aurorubens	Distance from Shore (km)			D/A

Table 3. Summary of significant predictors in models fitted to explain variation in abundance and encounter/non-encounter in the present study and Bolser et al. 2020. The generalized additive mixed models (GAMMs) from Bolser et al. 2020 were fit to data from all platforms displayed in Figure 1 and included random effects for site, survey team and visibility, as well as a tensor term between eastings and northings to account for spatial autocorrelation. The negative binomial and binomial generalized additive models (GAMs) developed in the present study were only fit to data with good water column visibility (average visibility score > 2.0/3.0; red colored platforms in Figure 1), and were also fit to data from one site visit by one survey team. A "+", "-", or "D" indicates that the predictor had a significant positive, negative, or domed relationship with a metric, respectively.
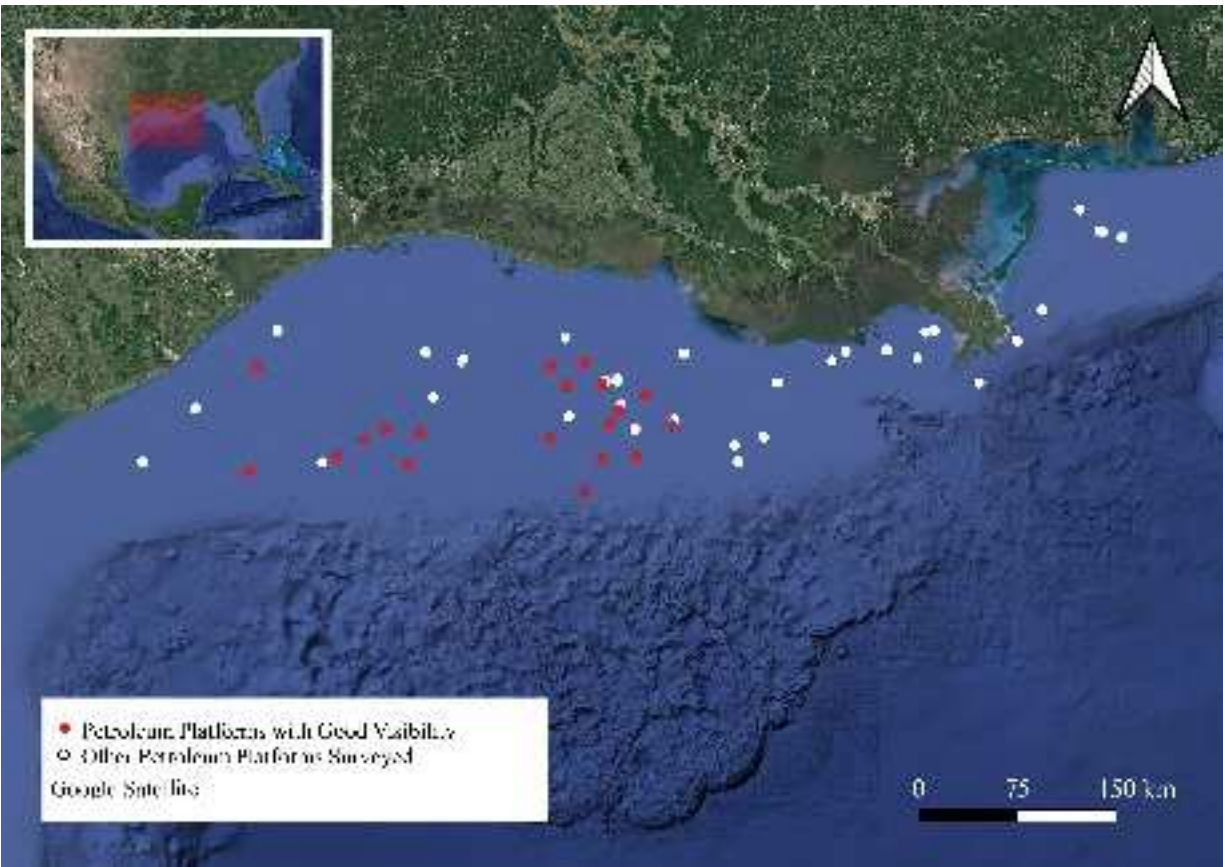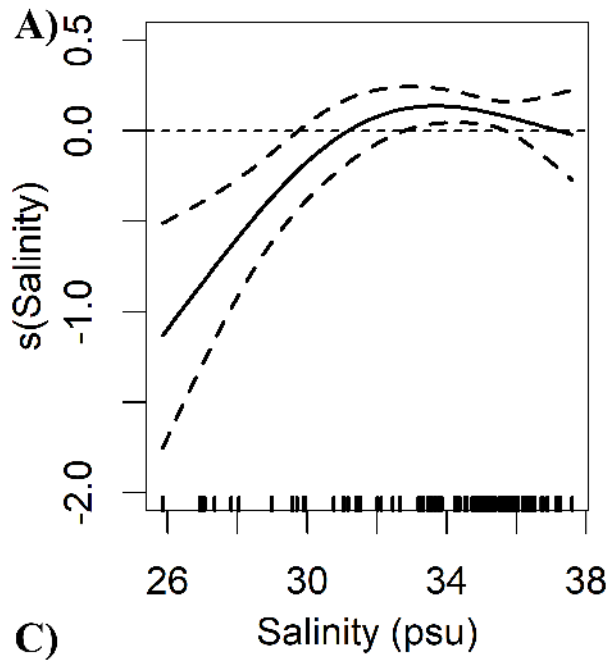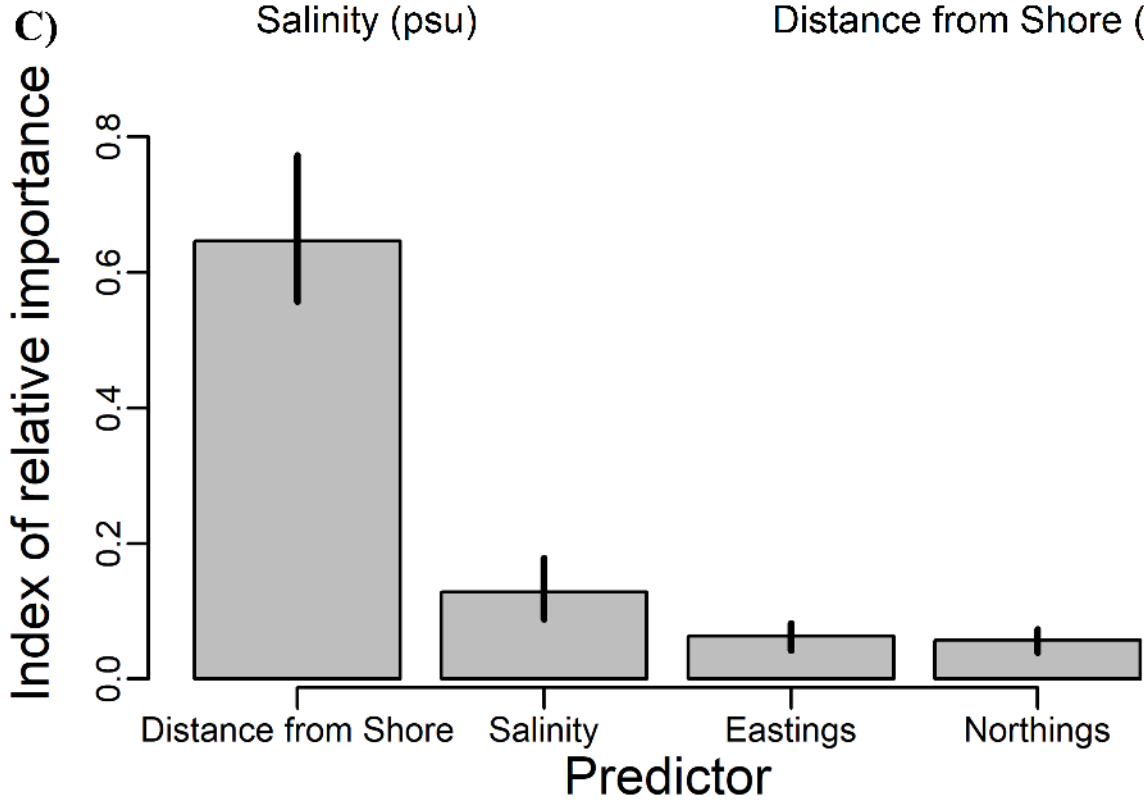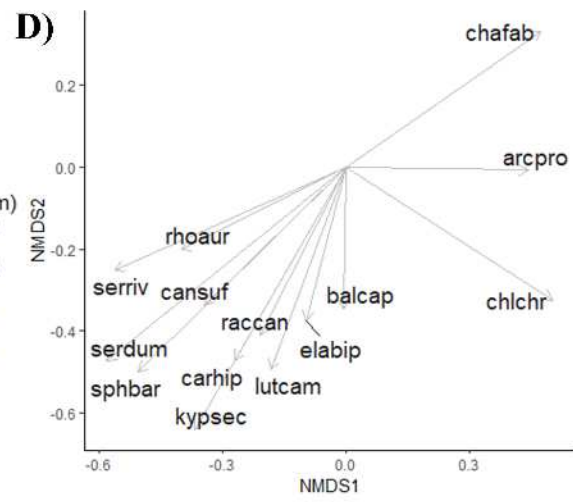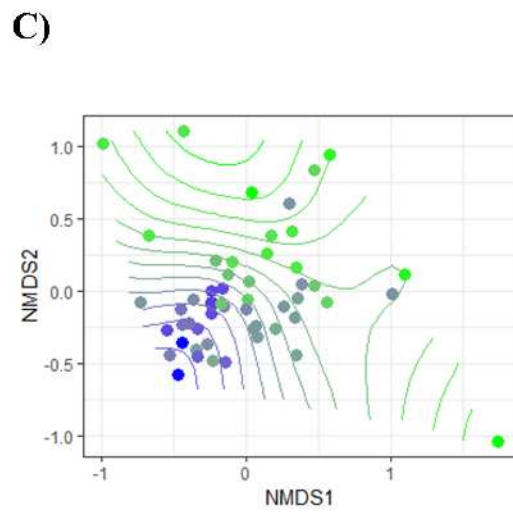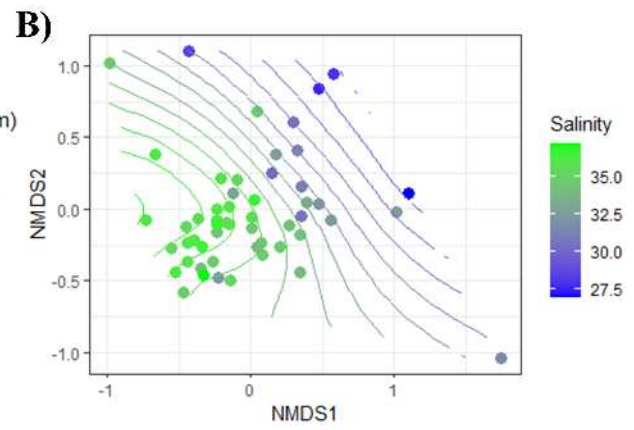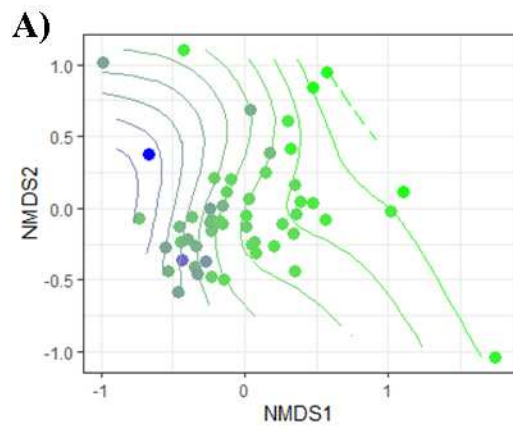
fsh_10654_f1.tif
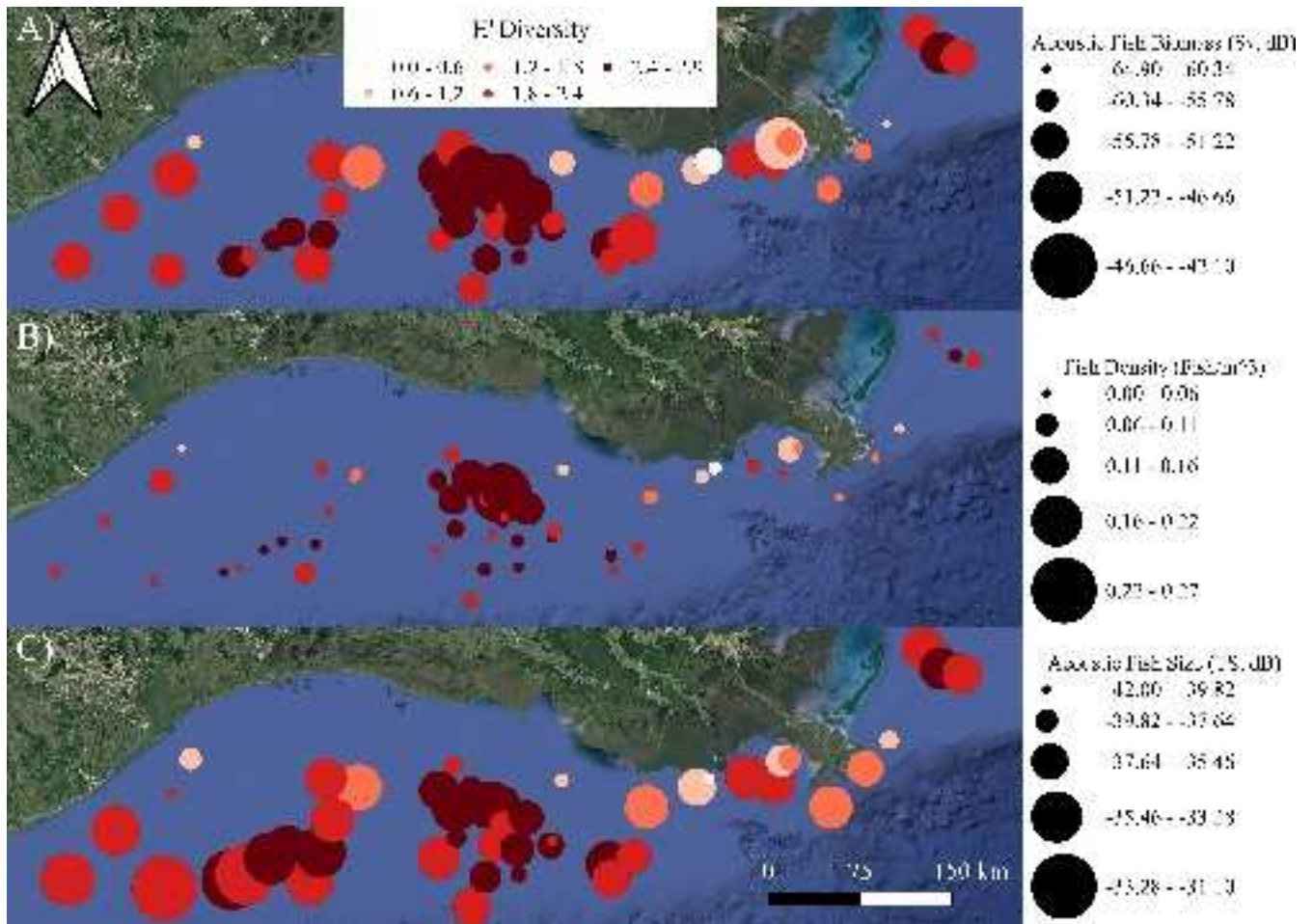
fsh_10654_f2.tiff
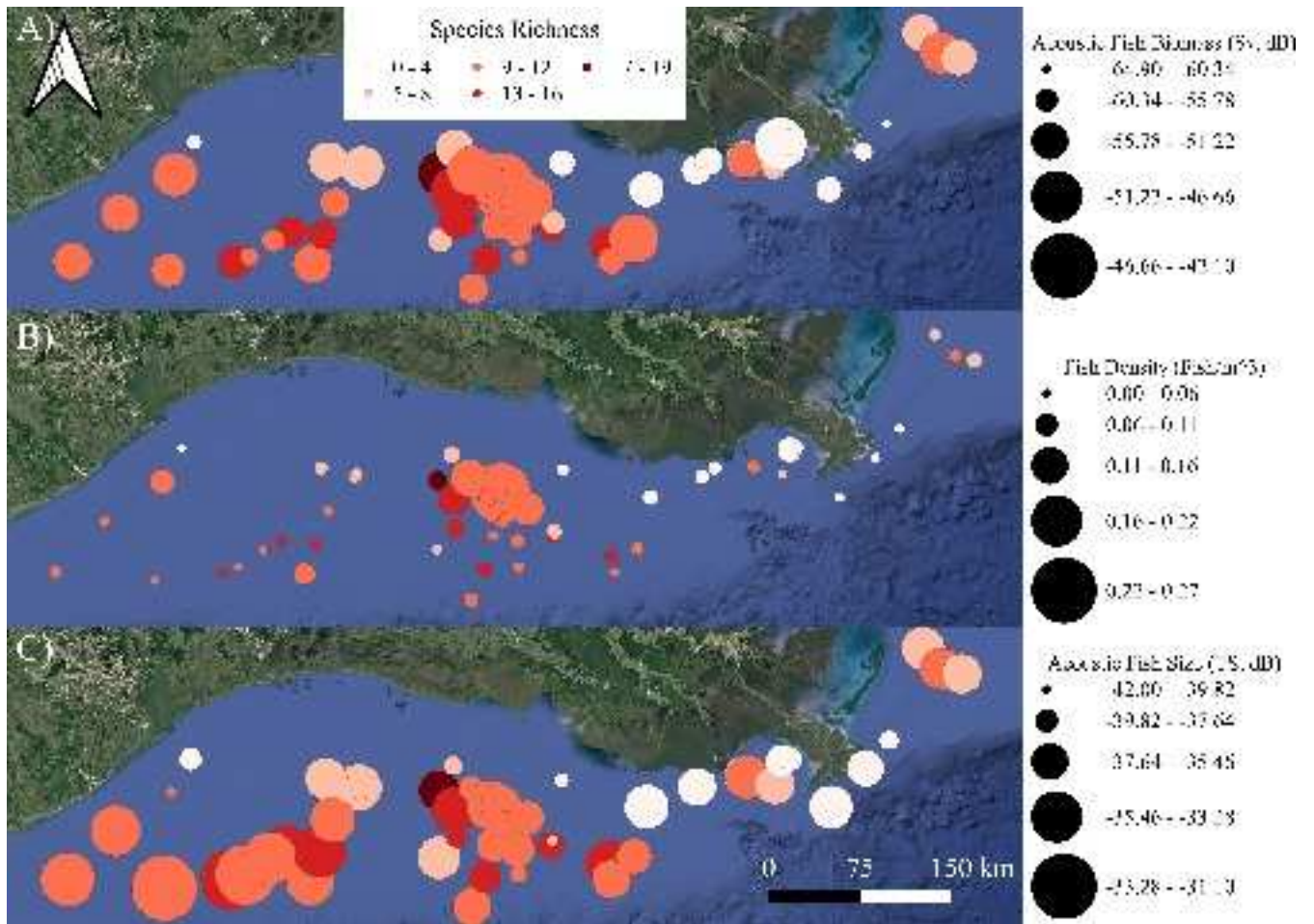
fsh_10654_f3.tiff
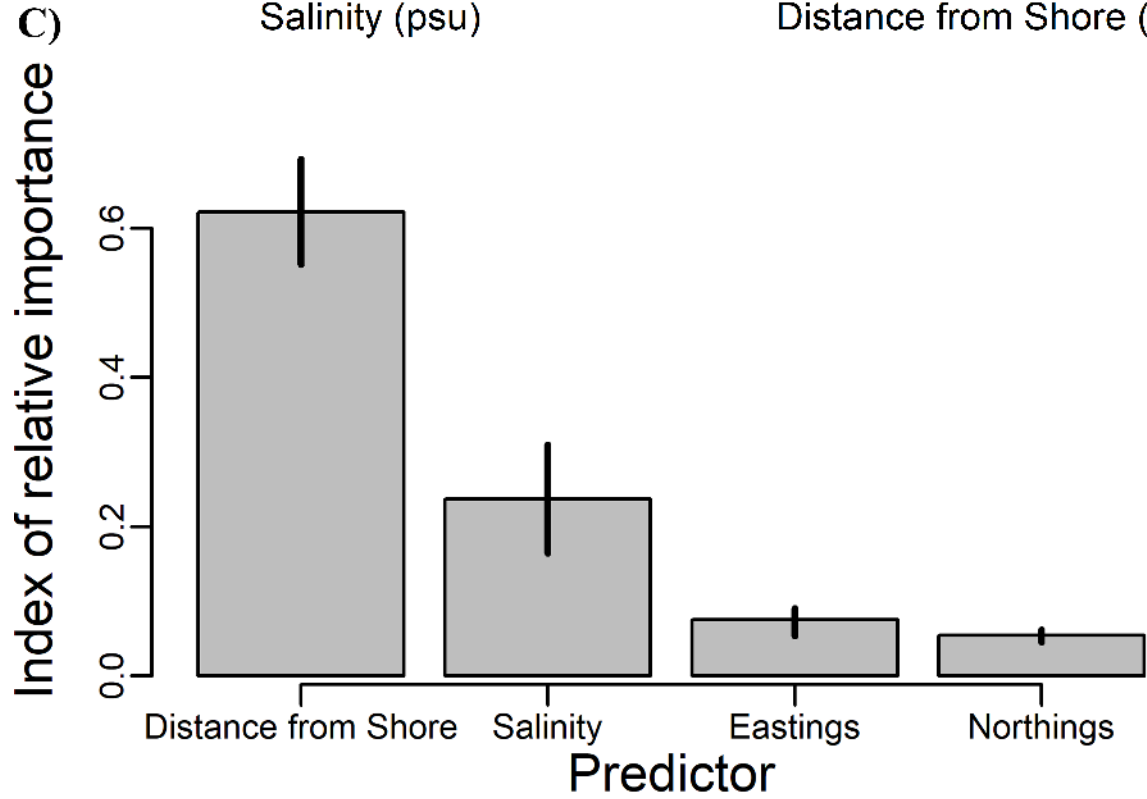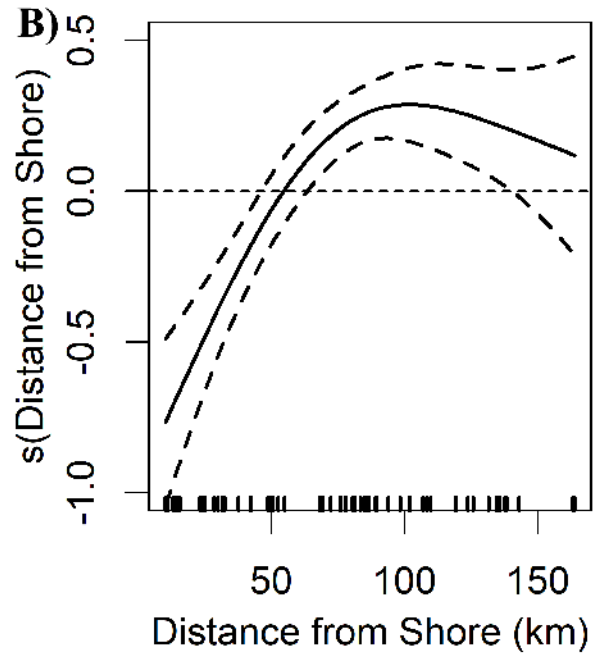
fsh_10654_f4.tif
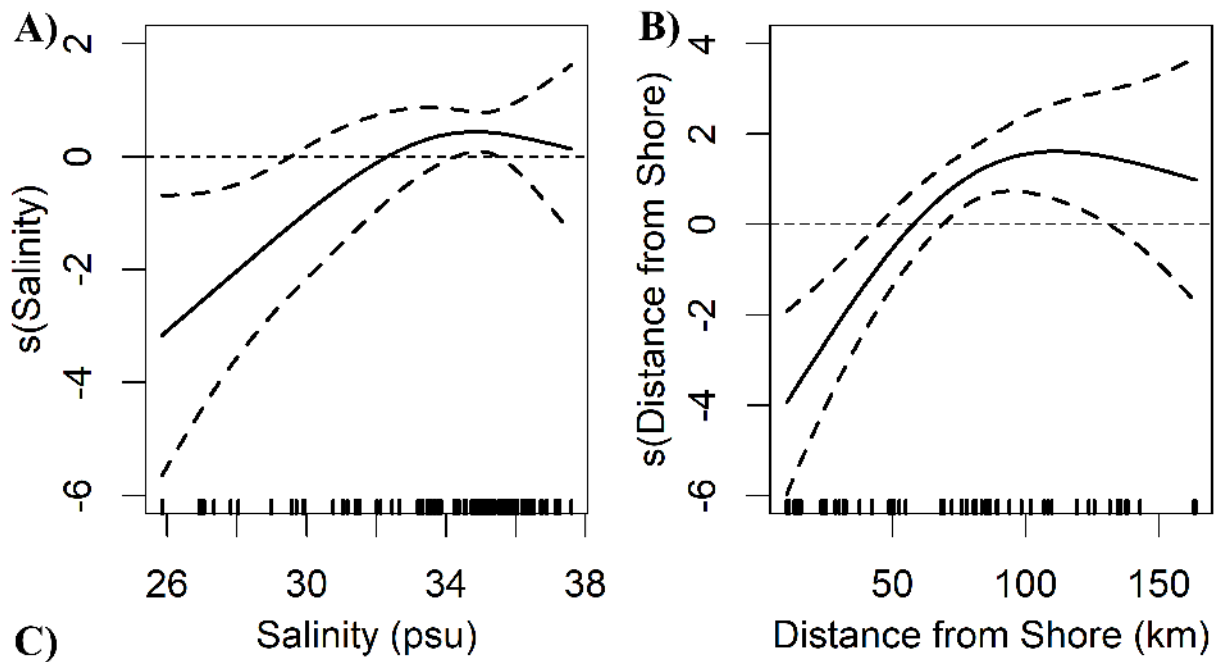
fsh_10654_f5.tif

fsh_10654_f6.tif